

Organo-Rare-Earth Complexes Supported by Chelating Diamide Ligands

Frank Estler, Georg Eickerling, Eberhardt Herdtweck, and Reiner Anwander*

Anorganisch-chemisches Institut, Technische Universität München, Lichtenbergstrasse 4, D-85747 Garching, Germany

Received September 18, 2002

The synthesis of a series of heteroleptic ate-complex-free rare-earth(III) diamide complexes by alkane and amine elimination reactions, starting from $\text{Ln}(\text{CH}_2\text{SiMe}_3)_3(\text{THF})_2$ and $\text{Ln}(\text{N}i\text{Pr}_2)_3(\text{THF})_x$ ($x = 1$, $\text{Ln} = \text{Sc}$, Lu ; $x = 2$, $\text{Ln} = \text{Y}$), respectively, is described. 2,6-Bis(((2,6-diisopropylphenyl)amino)methyl)pyridine ($\text{H}_2\text{BDPPpyr}$) formed monomeric complexes of the types $(\text{BDPPpyr})\text{Ln}(\text{CH}_2\text{SiMe}_3)(\text{THF})_x$ ($x = 1$, $\text{Ln} = \text{Sc}$, Lu ; $x = 2$, $\text{Ln} = \text{Y}$) and $(\text{BDPPpyr})\text{Ln}(\text{N}i\text{Pr}_2)(\text{THF})$ ($\text{Ln} = \text{Sc}$, Lu), which display enhanced stability for the smaller metal center scandium, for diisopropylamide coordination, and in donor solvents such as THF. Conversion of the silylalkyl complexes into their amide derivatives via secondary alkane elimination, i.e., reaction with HNEt_2 and $\text{HN}(\text{SiHMe}_2)_2$, increased the complex stability. The mono-THF adduct complexes $(\text{BDPPpyr})\text{Sc}(\text{L})(\text{THF})$ show a nonfluxional structure in solution, which contrasts the dynamic behavior of the corresponding bis-THF adduct complexes of the larger elements lutetium and yttrium. Sterically less encumbered 2,6-bis((mesitylamino)methyl)pyridine ($\text{H}_2\text{BMespyr}$) gave the less stable complexes $(\text{BMespyr})\text{Ln}(\text{CH}_2\text{SiMe}_3)(\text{THF})_x$ ($x = 1$, $\text{Ln} = \text{Sc}$; $x = 2$, $\text{Ln} = \text{Lu}$; the Y derivative could not be isolated). Again, subsequent silylalkyl/silylamide ligand exchange gave the complexes $(\text{BMespyr})\text{Ln}[\text{N}(\text{SiHMe}_2)_2](\text{THF})$, exhibiting considerably increased stability. The complexes $(\text{BDPPoxyl})\text{Ln}(\text{CH}_2\text{SiMe}_3)(\text{THF})$ ($\text{Ln} = \text{Sc}$, Lu , Y), derived from a nonfunctionalized diamide ligand ($\text{H}_2\text{BDPPoxyl} = 1,2\text{-bis-}(((2,6\text{-diisopropylphenyl)amino)methyl)benzene)$), were isolated in high yields. The 4- and 5-coordinate complexes $(\text{BDPPoxyl})\text{Sc}(\text{CH}_2\text{SiMe}_3)(\text{THF})$ and $(\text{BDPPpyr})\text{Sc}(\text{CH}_2\text{SiMe}_3)(\text{THF})$, respectively, were also characterized by X-ray diffraction structure determinations. All of the 5-coordinate scandium complexes derived from the BDPPpyr ligand effectively polymerize methyl methacrylate in a living manner ($M_w/M_n < 1.5$), affording mainly atactic polymer at ambient temperature.

Introduction

In the past decade “nonmetallocene” or “postmetallocene” complexes have attracted considerable attention in α -olefin polymerization chemistry.¹ Particularly, functionalized chelating diamide ligands have been extensively studied as a rigid supporting environment² giving highly active precatalysts comparable to the well-established group 4 metallocenes.³ The stereoelectronic demands of amide ligands can be effectively tuned by single or double functionalization of the coordinating nitrogen. For comparison, dialkoxide systems, which also implicate more electron-deficient metal centers, are sterically more difficult to control. Given the intrinsic interrelation between group 3/lanthanide and group 4 metal polymerization chemistry, corresponding “true” diamide complexes of the rare-earth metals have re-

ceived considerably less attention.^{4–12} Moreover, the polymerization efficiency of previously reported rare-earth complexes based on chelating diamide ligands seems to be limited,¹³ which is in contrast to the case for amidinate¹⁴ complexes as well as that for functionalized monoanionic amide complexes such as cationic triazacyclononane alkyls^{15,16} and amidodiphosphine alkyls.¹⁷

* To whom correspondence should be addressed. Fax: +49 89 289 13473. E-mail: reiner.anwander@ch.tum.de.

(1) Britovsek, G. J. P.; Gibson, V. C.; Wass, D. F. *Angew. Chem., Int. Ed.* **1999**, *38*, 428.

(2) (a) Schrock, R. R. *Acc. Chem. Res.* **1997**, *30*, 9. (b) Kempe, R. *Angew. Chem., Int. Ed.* **2000**, *39*, 468. (c) Gade, L. H. *Acc. Chem. Res.* **2002**, *35*, 575.

(3) For examples, see: (a) Guérin, F.; McConville, D. H.; Vittal, J. J. *Organometallics* **1996**, *15*, 5586. (b) Gibson, V. C.; Kimberley, B. S.; White, A. J. P.; Williams, D. J.; Howard, P. *Chem. Commun.* **1998**, 313.

(4) Gountchev, T. I.; Tilley, T. D. *Organometallics* **1999**, *18*, 2896.

(5) Cloke, F. G. N.; Elvidge, B. R.; Hitchcock, P. B.; Lamarche, V. M. E. *J. Chem. Soc., Dalton Trans.* **2002**, 2413.

(6) Shah, A. A. S.; Dorn, H.; Roesky, H. W.; Lubini, P.; Schmidt, H.-G. *Inorg. Chem.* **1997**, *36*, 1102.

(7) (a) Skinner, M. E. G.; Tyrrell, B. R.; Ward, B. D.; Mountford, P. *J. Organomet. Chem.* **2002**, *647*, 145. (b) Skinner, M. E. G.; Mountford, P. *J. Chem. Soc., Dalton Trans.* **2002**, 1694.

(8) Graf, D. D.; Davis, W. M.; Schrock, R. R. *Organometallics* **1998**, *17*, 5820.

(9) Fryzuk, M. D.; Yu, P.; Patrick, B. O. *Can. J. Chem.* **2001**, *79*, 1194.

(10) Lee, L.; Berg, D. J.; Bushnell, G. W. *Inorg. Chem.* **1994**, *33*, 5302.

(11) (a) Fryzuk, M. D.; Love, J. B.; Rettig, S. J. *J. Am. Chem. Soc.* **1997**, *119*, 9071. (b) Fryzuk, M. D.; Jafapour, L.; Kerton, F. M.; Love, J. B.; Patrick, B. O.; Rettig, S. J. *Organometallics* **2001**, *20*, 1387.

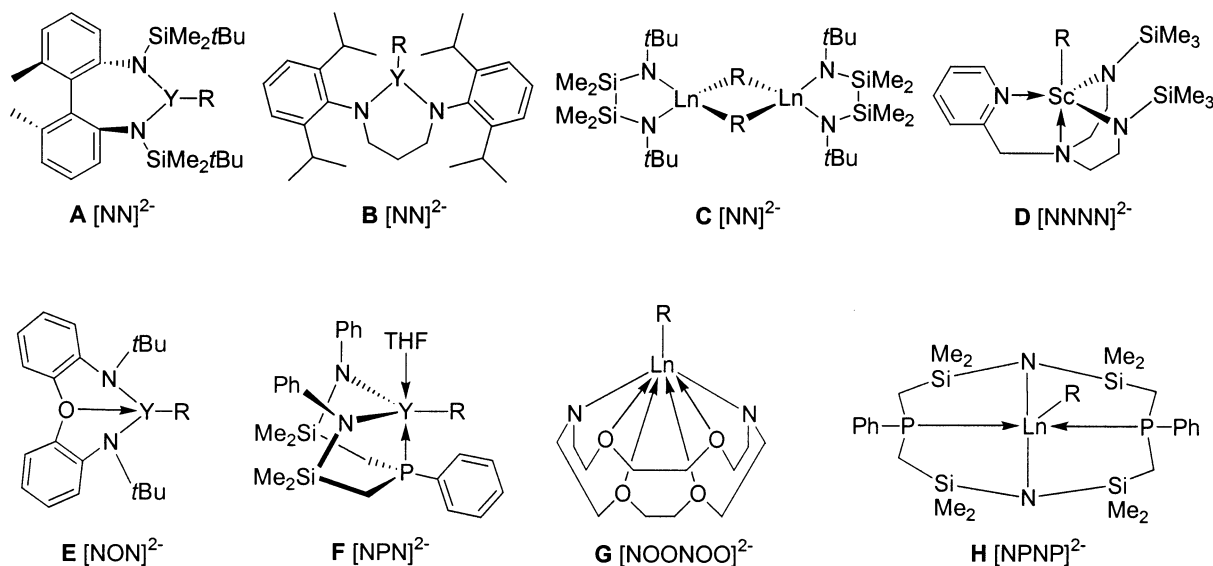
(12) Scholz, J.; Görls, H.; Schumann, H.; Weimann, R. *Organometallics* **2001**, *20*, 4394.

(13) Hou, Z.; Wakatsuki, Y. *Coord. Chem. Rev.* **2002**, *231*, 1.

(14) Duchateau, R.; van Wee, C. T.; Meetsma, A.; Teuben, J. H. J. *Am. Chem. Soc.* **1993**, *115*, 4931.

(15) Hajela, S.; Schaefer, W. P.; Bercaw, J. E. *J. Organomet. Chem.* **1997**, *532*, 45.

Chart 1



In their timely review article, Piers and Emslie presented a most useful classification of non-cyclopentadienyl ancillaries in organo-group 3 metal chemistry covering bi-, tri-, tetra-, and polydentate amide and alkoxide ligands.¹⁸ It is clearly seen that a rich chemistry has evolved from N-heteroallylic/electron-delocalized systems such as amidinates, guanidates, and aminotroponiminates as well as β -diketiminates, while true dianionic chelating diamide ligands seem to be underrepresented. For example, the C_2 -symmetric diamide complexes [DADMB]YR(THF)_x (A: DADMB = 2,2'-bis((*tert*-butyldimethylsilyl)amido)-6,6'-dimethylbiphenyl; R = H, Me, Et) (Chart 1) show no polymerization activity toward ethylene; however, rapid insertion of ethylene occurred for the hydride derivative to afford an yttrium ethyl complex.⁴ The B-type monoalkyl complex Y[ArN(CH₂)₃NAr]R (R = CH(SiMe₃)₂; Ar = C₆H₃/Pr₂-2,6) failed to undergo any 1-hexene insertion at elevated temperatures,⁵ while further "activation" of chloride and trifluoroacetate compounds of type C into hydride or alkyl derivatives has not yet been reported.⁶ Yttrium complexes of the types D,⁷ E,⁸ F,⁹ G,¹⁰ and H¹¹ carrying hard and soft donor substituted diamide ligands and an additional alkyl ligand were reported to be often unstable at ambient temperature or upon removal of coordinating solvent molecules such as THF. Remarkably, monoalkyl rare-earth-metal complexes of type H are capable of a nonradical/nonredox phenyl coupling.¹¹ In this paper, we wish to present the synthesis, structural characterization, and reactivity of various monoalkyl rare-earth complexes supported by bidentate and conformationally rigid tridentate diamide ligands. Their performance as initiators for acrylate polymerization reveals a remarkable structure-reactivity relationship.

Results and Discussion

Synthesis and Description of Diamine Ligand Precursors. Diamines 1–4 employed in this work were

prepared according to literature procedures (Chart 2).¹⁹ As the BDPPpyr ligand (1-2H; H₂BDPPpyr = 2,6-bis(((2,6-diisopropylphenyl)amino)methyl)pyridine) has been most successfully applied in group 4 and group 5 metal polymerization initiators,^{3a} we first set out to synthesize analogous rare-earth-metal complexes. This tridentate pincer ligand features two amide functions and a pyridine donor acting as a rigid backbone in derived metal complexes. The dianionic [NNN]²⁻ ligand has been shown to effectively stabilize five-coordinate complexes ligating exclusively in a meridional fashion.²⁰ The BMespyr ligand (2-2H; H₂BMespyr = 2,6-bis(((mesityl)amino)methyl)pyridine) was selected for reasons of decreased steric demand compared to ligand 1-2H. The methyl group at the 4-position was introduced to enhance its solubility in organic solvents. Furthermore, in contrast to its oily 2,6-bis(((2,6-dimethylphenyl)amino)methyl)pyridine (H₂BDMPpyr) analogue,²⁰ H₂BMespyr is easily obtained and purified as a solid. The previously unreported ligand BDPPmxy (3-2H; H₂BDPPmxy = 1,3-bis(((2,6-diisopropylphenyl)amino)methyl)benzene) was synthesized from α,α' -dibromo-*m*-xylene and lithium 2,6-diisopropylanilide. This "donor-free" analogue of BDPPpyr was anticipated to unravel the influence of the nitrogen donor on the structure, stability, and reactivity of the putative complexes. BDPPoxyl (4-2H; H₂BDPPoxyl = 1,2-bis(((2,6-diisopropylphenyl)amino)methyl)benzene) represents the bulkiest diamide ligand employed in this study. Its increased steric bulk obtained by aryl backbone 1,2-substitution should preferentially stabilize low-coordinate rare-earth alkyl complexes. Titanium(IV) complexes supported by this ligand were successfully used in isotactic propylene polymerization.²¹

Synthesis of Rare-Earth-Metal Precursors. Due to the *low acidity* of the diamine ligands under study, a transamination reaction according to our extended silylamide route was not feasible.²² Thus, we had to

(16) Bambirra, S.; van Leusen, D.; Meetsma, A.; Hessen, B.; Teuben, J. H. *Chem. Commun.* **2001**, 637.

(17) Fryzuk, M. D.; Giesbrecht, G.; Rettig, S. J. *Organometallics* **1996**, *15*, 3329.

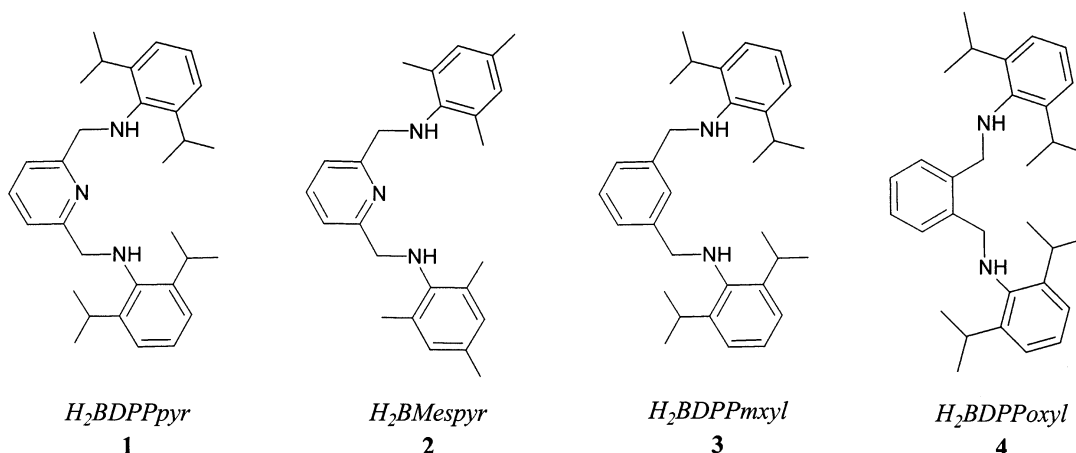
(18) Piers, W. E.; Emslie, D. J. H. *Coord. Chem. Rev.* **2002**, *233–234*, 131.

(19) Scollard, J. D.; McConville, D. H.; Vittal, J. J. *Organometallics* **1995**, *14*, 5478.

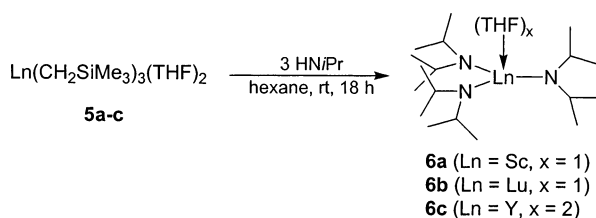
(20) (a) Guérin, F.; McConville, D. H.; Payne, N. C. *Organometallics* **1996**, *15*, 5085. (b) Guérin, F.; McConville, D. H.; Vittal, J. J. *Organometallics* **1997**, *16*, 1491.

(21) Tsubaki, S.; Jin, J.; Ahn, C.-H.; Sano, T.; Uozumi, T.; Soga, K. *Macromol. Chem. Phys.* **2001**, *202*, 482.

Chart 2

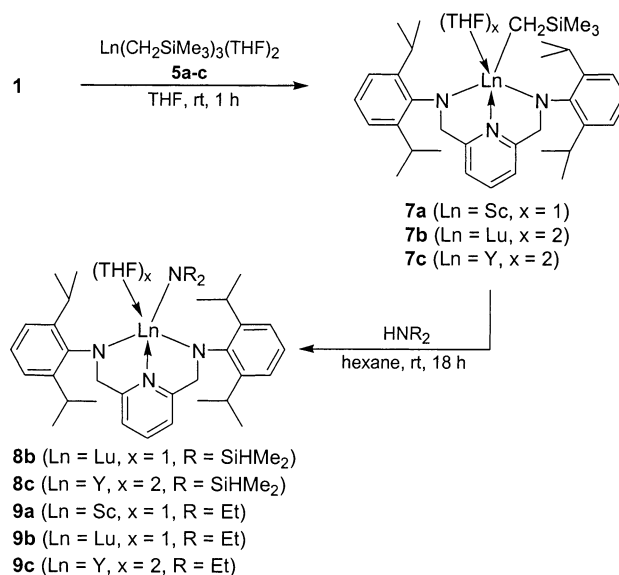


Scheme 1



focus on alternative lanthanide precursors exhibiting increased ligand basicity. To cover a reasonable reactivity scale, we decided to use lanthanide alkyls of the type $Ln(CH_2SiMe_3)_3(THF)_2$ ²³ and diisopropylamides of the type $Ln(NiPr)_3(THF)_x$.²⁴ The former silylalkyl complexes appeared in the literature as early as 1973 and have recently been used successfully in alkane elimination reactions.²⁵ The latter rare-earth diisopropylamides were first described by Ghotra and Hart.²⁴ However, their original synthesis according to a "conventional" salt metathesis reaction involving lithium diisopropylamide (LDA) and rare-earth halides as well as variations therefrom led exclusively to mixtures of $Ln(NiPr)_3(THF)_x$ and their corresponding ate complexes $MLn(NiPr)_4(THF)_x$ ($M = Li, Na$),²⁶ impeding their use as valuable synthetic precursors. Here we describe the synthesis of the first ate-complex-free lanthanide tris-(diisopropylamide) complexes utilizing the lanthanide alkyls described above (Scheme 1). Reaction of $Ln(CH_2SiMe_3)_3(THF)_2$ (**5**) with 3 equiv of diisopropylamine in hexane at room temperature for 18 h produced $Ln(NiPr)_3(THF)_x$ (**6**) in high yields ($x = 1$; $Ln = Sc, Lu$; $x = 2$, $Ln = Y$). The solid-state connectivity structure of yttrium derivative **6c** revealed a mononuclear bis-THF

Scheme 2



adduct with severely disordered amide and THF ligands.²⁷ Such rare-earth amide precursors should be basic enough to deprotonate the aryl-substituted diamine ligands **1–4**. The resulting heteroleptic complexes $LLn(NiPr)_2$ could display enhanced stability compared to the corresponding heteroleptic silylalkyl complexes due to the increased steric bulk of the diisopropylamide ligand.

Synthesis of Diamide Complexes Derived from BDPPpyr. Reaction of $H_2BDPPpyr$ (**1**, Chart 2) with $Ln(CH_2SiMe_3)_3(THF)_2$ in THF at ambient temperature for 1 h yielded the monoalkyl complexes **7a–c**. Spectroscopic and microanalytical data are consistent with a molecular composition as shown in Scheme 2: that is, a five-coordinate mono-THF adduct for the scandium derivative **7a** and a six-coordinate bis-THF adduct for the larger metal centers lutetium (**7b**) and yttrium (**7c**). The stability of the complexes decreases with increasing size of the metal center. While scandium complex **7a** is stable in noncoordinating solvents such as hexane, compounds **7b,c** undergo slow (within 1 day) and rapid

(22) Anwander, R. *Top. Organomet. Chem.* **1999**, 2, 1.

(23) (a) Lappert, M. F.; Pearce, R. *J. Chem. Soc., Chem. Commun.* **1973**, 126. (b) Arndt, S.; Voth, P.; Spaniol, T. P.; Okuda, J. *Organometallics* **2000**, 19, 4690.

(24) Bradley, D. C.; Ghotra, J. S.; Hart, F. A. *Inorg. Nucl. Chem. Lett.* **1976**, 12, 735.

(25) (a) Mu, Y.; Piers, W. E.; MacQuarrie, D. C.; Zawarotko, M. J.; Young, U. G., Jr. *Organometallics* **1996**, 15, 2720. (b) Hultsch, K. C.; Spaniol, T. P.; Okuda, J. *Angew. Chem., Int. Ed.* **1999**, 38, 227. (c) Hultsch, K. C. Ph.D. Thesis, Johannes Gutenberg-Universität Mainz, 1999. (d) Hultsch, K. C.; Okuda, J.; Voth, P.; Beckerle, K.; Spaniol, T. P. *Organometallics* **2000**, 19, 228. (e) Evans, W. J.; Brady, J. C.; Ziller, J. W. *J. Am. Chem. Soc.* **2001**, 123, 7711. (f) Emslie, D. J. H.; Piers, W. E.; Parvez, M.; McDonald, R. *Organometallics* **2002**, 21, 4226.

(26) (a) Aspinall, H. C.; Tillotson, M. R. *Polyhedron* **1994**, 13, 3229. (b) Evans, W. J.; Anwander, R.; Ziller, J. W.; Khan, S. I. *Inorg. Chem.* **1995**, 34, 5927.

(27) Due to strong ligand disordering in the solid state at 143 K only the atomic connectivity of the compound could be unambiguously determined. **6c** crystallized from hexane in the orthorhombic space group $Cmc2_1$ (No. 36) with $a = 12.9407(4)$ Å, $b = 14.862(1)$ Å, $c = 16.1536(7)$ Å, $V = 3106.7(3)$ Å³, and $D_{\text{calcd}} = 1.141$ g cm⁻³ for $Z = 4$.

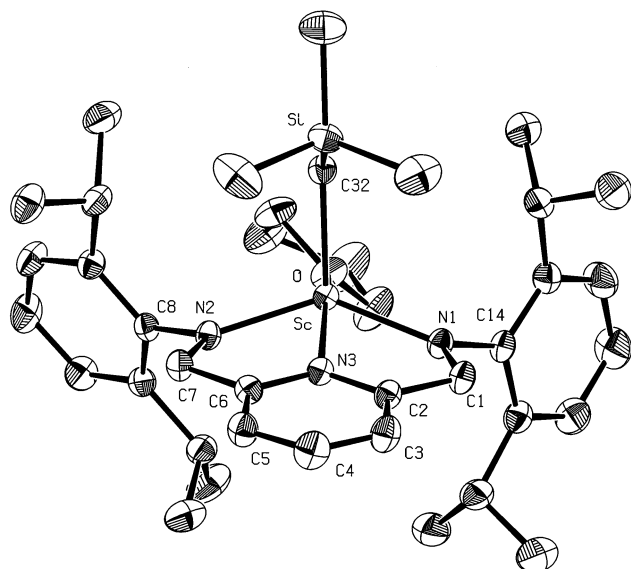


Figure 1. PLATON⁴⁶ drawing of the complex (BDPPpyr)-ScCH₂SiMe₃(THF) (**7a**) in the solid state. Thermal ellipsoids are drawn at the 50% probability level. The unit cell contains one molecule of toluene, which is omitted for clarity.

decomposition (within 1 h), respectively. A pronounced instability of diamide complexes in the absence of coordinating solvent molecules such as THF has been pointed out previously.^{8,10,18}

The ¹H NMR spectrum of **7a** in C₆D₆ revealed a nonfluxional coordination at ambient temperature. The diastereotopic *N*-methylene groups exhibit two doublets at 5.41 and 4.46 ppm, which are considerably downfield shifted compared to those of **1** (δ 4.26 ppm). The isopropyl groups of the conformationally rigid [NNN]²⁻ ligand also exhibit one significantly downfield shifted multiplet for the methine groups at 4.54 ppm and one slightly upfield shifted multiplet at 3.43 ppm (cf., H₂-BDPPpyr, δ = 3.54 ppm) as well as four doublets for the methyl groups at 1.53, 1.45, 1.15, and 1.14 ppm, respectively. This indicates a large rotational barrier for the isopropyl groups, making them diastereotopic. The signals of the lutidine ring appear upfield shifted at 6.94 and 6.60 ppm, respectively, indicating an interaction between the lutidine and the metal center (cf. H₂-BDPPpyr, δ 7.05 and 6.85 ppm). Moreover, the significantly upfield shifted multiplets of the THF ligand at 3.01 and 0.78 ppm are in agreement with a strongly bonded THF molecule.

An X-ray structure analysis of complex **7a** confirmed its mononuclear nature and composition, as shown in Scheme 2. A view of the molecular structure and relevant bond distances and angles can be found in Figure 1 and Table 1.

The coordination geometry at the five-coordinate scandium metal center is best described as distorted trigonal bipyramidal. The anilide nitrogen atoms (N1, N2) and the alkyl ligand (C32) form the equatorial plane, while the THF oxygen atom and the pyridine nitrogen atom (N3) occupy the apical positions (O–Sc–N3 = 156.01(5)°). The [NNN]²⁻ ligand coordinates in a meridional fashion with a bite angle of 137.04(6)°, which is a typical coordination mode for this pincer ligand, as previously shown for Ti(IV), Zr(IV), and Ta(V) complexes.^{3a,19,20}

Table 1. Selected Bond Lengths (Å) and Angles (deg) for Complex **7a**

Sc–N1	2.101(2)	Sc–O	2.182(1)
Sc–N2	2.092(1)	Sc–C32	2.248(2)
Sc–N3	2.219(1)		
N1–Sc–N2	137.04(6)	O–Sc–N3	156.01(5)
N1–Sc–N3	72.22(5)	C32–Sc–N1	109.35(6)
N2–Sc–N3	72.75(5)	C32–Sc–N2	104.39(6)
O–Sc–C32	96.21(6)	C32–Sc–N3	107.71(6)
O–Sc–N1	101.97(5)	Sc–C32–Si	123.63(9)
O–Sc–N2	99.96(5)		

The Sc–N1/N2 bond lengths of 2.097 Å (average) are considerably longer than those in four-coordinate Sc[N(SiHMe₂)₂]₃(THF) (2.069 Å (average)).²⁸ For comparison, the Sc–N distances in five-coordinate dialkylscandium complexes supported by a β -diketiminato ligand are 2.190(7) and 2.201(6) Å.²⁹ The Sc–O(THF) and Sc–N(lutidine) donor bond lengths of 2.182(1) and 2.219(1) Å lie in the expected range. The Sc–C(alkyl) bond distance, 2.248(2) Å, is comparable to those of the formerly mentioned β -diketiminato complex, 2.210(9) and 2.245(9) Å.²⁹ Sc–C bond lengths for other neutral monoalkyl complexes range from 2.243(8) to 2.346(2) Å.^{30–33}

The ¹H NMR spectrum of **7b** in C₆D₆ shows a set of resonances comparable to those for **7a**, except for the lutidine ring and the alkyl ligand, whose broad signals indicate rapid structural fluctuation. For example, the *N*-methylene groups display two broad singlets at 5.42 and 4.57 ppm. We ascribe the observed fluxional solution structure to (i) a weak metal–THF interaction and facile THF dissociation, which is corroborated by the slight shift of the THF signal compared to noncoordinated THF, and (ii) to a poor coordinative fit of the [NNN]²⁻ ligand with larger metal centers, involving labile Ln–N bonds and probably intermolecular Ln–N association. Since both this fluctuation and complex decomposition increase with increasing size of the metal center, we could not obtain an interpretable ¹H NMR spectrum of yttrium derivative **7c** in C₆D₆. The dynamic behavior of complexes **7b,c** is supported by their ¹H NMR spectra in THF-*d*₈. In those spectra, the *N*-methylene groups display significantly downfield shifted singlets at 4.95 (**7b**) and 4.87 (**7c**) ppm (cf., δ (**1**, THF-*d*₈) 4.19 ppm), suggesting a C₂-symmetric ligand sphere for a bis-THF adduct. The signals of the aryl-bonded isopropyl groups, which are multiplets at 3.84 (**7b**) and 3.80 (**7c**) ppm (cf. δ (**1**, THF-*d*₈) 3.49 ppm) and two doublets at 1.16/1.14 (**7b**) and 1.17/1.15 ppm (**7c**) (cf. δ (**1**, THF-*d*₈) 1.21 ppm), indicate enhanced steric saturation via a large rotational barrier for the isopropyl groups, making them diastereotopic.

Complexes **7a–c** feature one remaining alkyl ligand accessible to secondary ligand exchange reactions. We

(28) Anwander, R.; Runte, O.; Eppinger, J.; Gerstberger, G.; Herdtweck, E.; Spiegler, M. *J. Chem. Soc., Dalton Trans.* **1998**, 847.

(29) Hayes, P. G.; Piers, W. E.; Lee, L. W. M.; Knight, L. K.; Parvez, M.; Elsegood, M. R. J.; Clegg, W. *Organometallics* **2001**, 20, 2533.

(30) Thompson, M. E.; Baxter, S. M.; Bulls, A. R.; Burger, B. J.; Nolan, M. C.; Santarsiero, B. D.; Schaefer, W. P.; Bercaw, J. E. *J. Am. Chem. Soc.* **1987**, 109, 203.

(31) Schaefer, W. P.; Köhn, R. D.; Bercaw, J. E. *Acta Crystallogr.* **1992**, C48, 251.

(32) Arnold, J.; Hoffmann, C. G.; Dawson, D. Y.; Hollander, F. J. *Organometallics* **1993**, 12, 3645.

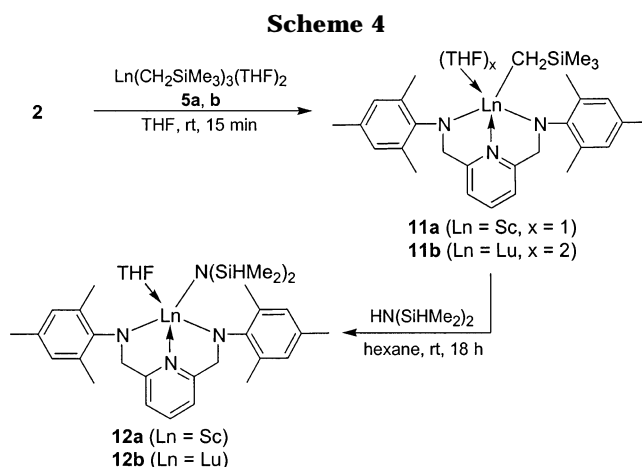
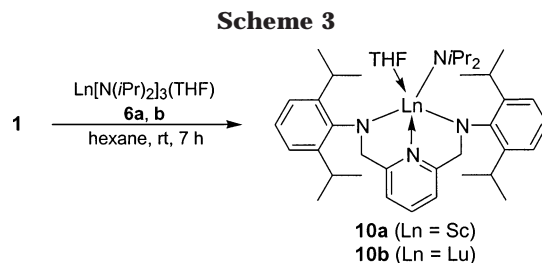
(33) Schumann, H.; Erbsstein, F.; Herrmann, K.; Demtschuk, J.; Weimann, R. *J. Organomet. Chem.* **1998**, 562, 255.

examined the reactivity of **7a–c** toward tetramethyldisilazane ($\text{HN}(\text{SiHMe}_2)_2$), diethylamine, and diisopropylamine, as shown in Scheme 2. Such envisaged heteroleptic triamido complexes should be more stable than complexes **7** but still reactive enough for further derivatization involving the terminally bonded amide ligand.

Reaction of **7a–c** with $\text{HN}(\text{SiHMe}_2)_2$ in hexane at ambient temperature for 18 h gave the silylamide derivatives **8b** (Lu) and **8c** (Y). The scandium analogue **8a** did not form even after a 48 h reaction period, probably due to steric reasons. Spectroscopic and microanalytical data are consistent with five- (**8b**) or six-coordinate complexes (**8c**). For the mono-THF adduct **8b**, a nonfluxional structure is found in C_6D_6 with both diastereotopic *N*-methylene and aryl-bonded isopropyl groups as well as a strong *N*(lutidine) and *O*(THF) donor bonding. The spectroscopic features of the $\text{N}(\text{SiHMe}_2)_2$ ligand are Si–H stretching vibrations at ν 2103 and 2042 cm^{-1} and a SiH proton resonance at 4.64 ppm (septet). Because of rapid THF fluctuation in the yttrium bis-THF adduct **8c** (cf. **7b,c**) its NMR spectra were recorded in $\text{THF}-d_8$. The singlet resonance of the *N*-methylene groups at 4.78 ppm indicates a symmetric ligand sphere, while the signals of the aryl-bonded isopropyl methyl groups, displaying a multiplet at 3.67 ppm and two doublets at 1.18/1.12 ppm, are diastereotopic as a consequence of restricted rotation about the $\text{N}-\text{C}_{\text{ipso}}$ bond. The presence of a $\text{N}(\text{SiHMe}_2)_2$ ligand in **8c** is clearly indicated by the Si–H stretching vibration at ν 2097 and 2010 cm^{-1} and a SiH proton displaying a septet at δ 4.46 ppm.

The HNEt_2 reaction (Scheme 2), which was conducted for **7a–c** in hexane at ambient temperature for 18 h, gave ligand exchange for all complexes. Spectroscopic data and elemental analyses are consistent with the formation of a mono-THF adduct for scandium (**9a**) and lutetium (**9b**) and a six-coordinate bis-THF adduct for yttrium (**9c**). The handling of complexes **9a–c** revealed an increased stability compared to those of complexes **7a–c**.³⁴ ^1H NMR spectroscopy of diethylamido complexes **9a,b** showed the absence of any dynamic behavior in C_6D_6 . Again, the familiar signal pattern for both diastereotopic *N*-methylene groups and isopropyl methyl groups was observed. Donor moieties strongly interacting with the metal centers are indicated by the upfield shifted lutidine ring signals and upfield shifted THF multiplets. For reasons of facile donor (THF) dissociation, the ^1H NMR spectrum of the yttrium bis-THF adduct **9c** was measured in $\text{THF}-d_8$. The C_2 symmetry of complex **9c** is evidenced by a sharp resonance for the *N*-methylene groups at 4.77 ppm. Again, inequivalent isopropyl groups are consistent with a hindered rotation about the $\text{N}-\text{C}_{\text{ipso}}$ bond.

With HNiPr_2 no ligand exchange reactions could be observed in hexane at ambient temperature after a period of 18 h. We interpret this as a consequence of the relatively lower Brønsted acidity of HNiPr_2 vs $\text{HN}(\text{SiHMe}_2)_2$ combined with the increased steric demand (HNiPr_2 vs HNEt_2). However, the diisopropylamide derivatives **10a,b** were obtained from $\text{Ln}(\text{N}(\text{iPr})_2)_3(\text{THF})_x$ (**6**) and 1 equiv of $\text{H}_2\text{BDPPpyr}$ in hexane at ambient



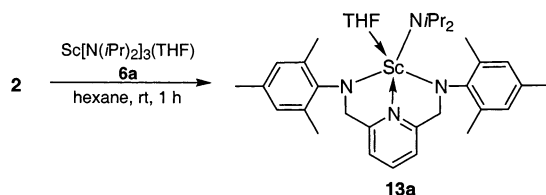
temperature after 7 h (Scheme 3). Complexes **10a,b** are stable in noncoordinating solvents such as hexane.

The ^1H NMR spectrum of **10a** recorded in C_6D_6 revealed a signal set comparable to that of **7a**; however, as for complex **7b** broad signals were observed, which is in agreement with a weakly coordinated THF ligand. For example, the *N*-methylene groups of **10a** show two very broad singlets at approximately 5.4 and 4.5 ppm. An interpretable NMR spectrum of **10b** in C_6D_6 was not obtained. The NMR spectra of **10a,b** simplified remarkably when recorded in a donor solvent such as $\text{THF}-d_8$. Now, the *N*-methylene groups feature a significantly downfield shifted singlet at 4.74 (**10a**) and 4.85 ppm (**10b**), implicating a higher complex symmetry.

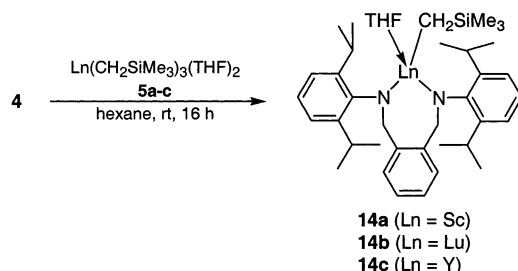
Synthesis of Diamide Complexes Derived from BMespyr. Reaction of the complexes $\text{Ln}(\text{CH}_2\text{SiMe}_3)_3(\text{THF})_2$ with 1 equiv of $\text{H}_2\text{BMespyr}$ (**2**; Chart 2) in THF at ambient temperature for 15 min gave complexes **11a,b** (Scheme 4). Remarkably, the putative complex **11c** derived from the larger yttrium metal could not be isolated, which we interpret as a consequence of a very fast decomposition. Spectroscopic data and elemental analyses of **11a,b** are consistent with a mono-THF and a bis-THF adduct, respectively. The complexes are stable in donor solvents only, and again, the stability of the complexes decreases with increasing size of the metal center. ^1H NMR spectroscopy in $\text{THF}-d_8$ revealed a symmetric ligand environment. The *N*-methylene groups were found as significantly downfield shifted singlets at 4.72 (**11a**) and 4.85 ppm (**11b**) (cf. $\delta(\text{H}_2\text{-BMespyr}, \text{THF}-d_8)$ 4.22 ppm). The aryl-bonded methyl groups exhibit two singlets at 2.24 and 2.16 ppm (**11a**) and 2.26 and 2.15 ppm (**11b**), respectively. These findings are in good agreement with those obtained for the BDPPpyr complexes. The sterically less encumbered BMespyr ligand implies shorter reaction times and increased steric unsaturation at the metal centers. While the yttrium derivative **7c** of the bulkier BDPPpyr

(34) Complex **9a** was also synthesized from hexane-soluble $[\text{Sc}(\text{NEt}_2)_3]$ and **1**.

Scheme 5



Scheme 6



ligand is isolable, the corresponding BMespyr complex is unstable at ambient temperature.

On the other hand, BMespyr complexes **11a,b** can be further stabilized via alkane elimination and formation of complexes (BMespyr)LnN(SiHMe₂)₂(THF) (Ln = Sc (**12a**), Ln = Lu (**12b**); Scheme 4). Complexes **12** are even stable in noncoordinating solvents, wherein the scandium mono(THF) adduct **12a** shows a nonfluxional structure featuring a relatively strong interaction between the lutidine and the metal center. The N(SiHMe₂)₂ ligand is characterized by Si–H stretching vibrations at ν 2075 and 1920 cm^{−1} and a SiH proton displaying a septet at δ 4.83 ppm. Because of rapid THF fluctuations in C₆D₆ at ambient temperature, conclusive NMR spectra of **12b** were obtained only in THF-*d*₈. The spectroscopic features of the N(SiHMe₂)₂ ligand are a Si–H stretching vibration at ν 2062 cm^{−1} and a SiH proton displaying a septet at δ 4.34 ppm.

Addition of 1 equiv of H₂Mespyr to Sc(N \overline{P} Pr₂)₃(THF) in hexane at ambient temperature afforded complex **13a** after 1 h (Scheme 5). Like its silylamide analogue **12a**, complex **13a** is stable in noncoordinating solvents. ¹H NMR spectroscopy of **13a** in THF-*d*₈ revealed a significantly downfield shifted singlet at 4.63 ppm for the *N*-methylene groups consistent with a symmetric ligand sphere.

Attempted Synthesis of Diamide Complexes Derived from BDPP α myl. Under the reaction conditions, which have been successfully applied for the synthesis of BDPPpyr and BMespyr rare-earth complexes, the N-donor-free analogue H₂BDPP α myl (**3**; Chart 2) did not form any tractable product. For example, when **3** was reacted with Ln(CH₂SiMe₃)₃(THF)₂ in hexane or THF at ambient temperature, the formation of the putative complexes (BDPP α myl)Ln(CH₂SiMe₃)(THF)_x did not occur after 2 h. Also, prolonged reaction times led to decomposition or oligomerization products only. This observation can be explained by a strongly stabilizing effect of the central lutidine donor atom on the eight-membered metallacycles in BDPPpyr- and BMespyr-derived complexes.

Synthesis of Diamide Complexes Derived from BDPP α myl. Reaction of the *o*-xylene-derived diamine H₂BDPP α myl (**4**; Chart 2) with Ln(CH₂SiMe₃)₃(THF)₂ in

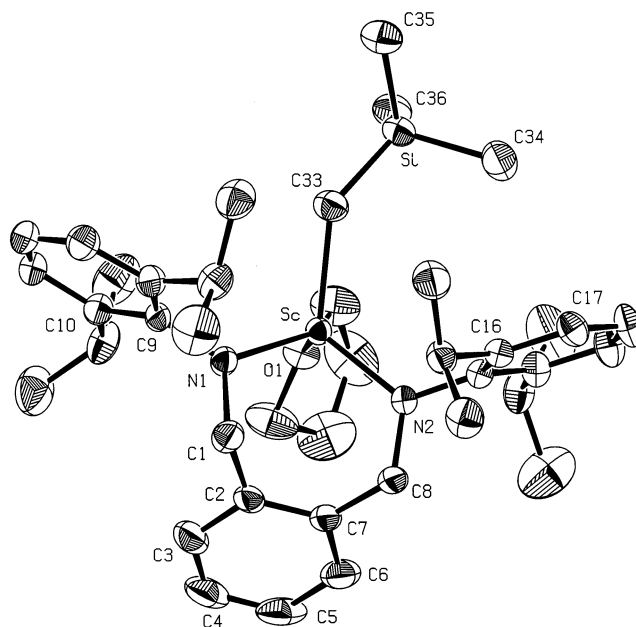


Figure 2. PLATON⁴⁶ drawing of the complex (BDPP α myl)-ScCH₂SiMe₃(THF) (**14a**) in the solid state. Thermal ellipsoids are drawn at the 50% probability level.

Table 2. Selected Bond Lengths (Å) and Angles (deg) for Complex **14a**

Sc–N1	2.017(1)	Sc–O1	2.161(1)
Sc–N2	2.037(1)	Sc–C33	2.218(2)
N1–Sc–N2	105.79(5)	O1–Sc–N1	109.74(6)
N1–Sc–C33	106.73(7)	O1–Sc–N2	108.73(5)
N2–Sc–C33	118.30(7)	Sc–C33–Si	137.4(1)
O1–Sc–C33	107.37(6)		

hexane at ambient temperature for 16 h gave the diamide complexes **14a–c** in quantitative yields (Scheme 6). Apparently, the ortho-substituted ligand backbone provides a sterically preferred environment, giving seven-membered metallacycles of increased stability compared to putative **3**-derived complexes featuring the meta-substituted ligand backbone. Spectroscopic and microanalytical data are consistent with the formation of monoalkyl complexes carrying an additional THF ligand. Such four-coordinate heteroleptic complexes are stable in nondonor solvents.

¹H NMR spectroscopy of **14a** in C₆D₆ revealed diastereotopic *N*-methylene groups appearing as two considerably downfield shifted doublets at 5.52 and 3.64 ppm. A marked rotational barrier about the N–C_{ipso} bond is evidenced by two downfield shifted multiplets at 4.26 and 3.55 ppm for the isopropyl methine groups and by four doublets at 1.62, 1.55, 1.34, and 1.16 ppm for the isopropyl methyl groups. Two significantly upshifted multiplets at 3.28 and 1.15 ppm indicate a strongly bonded THF molecule.

The solid-state structure of complex **14a** could be unequivocally established by an X-ray structure analysis (Figure 2). The scandium center adopts a distorted-tetrahedral geometry. Selected bond distances and angles are given in Table 2. The BDPP α myl ligand shows a bite angle of 105.79(5)°. The Sc–N bond lengths average 2.027 Å and, as expected, are markedly shorter than those in the five-coordinate complex **7a**; however, they are also considerably shorter than those in four-coordinate dialkylscandium complexes supported by a

β -diketiminato ligand (2.091(5)–2.145(1) Å).²⁹ The Sc–C bond length of 2.218(2) Å is similar to those in the aforementioned β -diketiminato complex (2.118(5)–2.265(6) Å)²⁹ and that in (N₂NN')Sc(CH₂SiMe₃) (2.289(2) Å; H₂N₂NN' = (2-C₅H₄N)CH₂N{CH₂CH₂N(H)SiMe₃}₂).⁷

The ¹H NMR spectra of **14b,c** were measured in THF-*d*₈ because of THF fluctuations occurring in C₆D₆. The singlet for the *N*-methylene groups, which appears significantly downfield shifted at 4.65 (**14b**) and 4.69 ppm (**14c**) (cf. δ (**4**, THF-*d*₈) 4.15 ppm), indicates a symmetric ligand sphere. The xylene ring exhibits significantly upfield shifted multiplets at 7.1–6.9 ppm (**14b**) and 7.1–6.8 ppm (**14c**) (cf. δ (**4**, THF-*d*₈) 7.55/7.25 ppm) indicative of an interaction between the aromatic system and the metal center. It is interesting to note that the accessibility and stability of five- and four-coordinate complexes derived from BDPPpyr and BDPPoxyl ligands, respectively, are very similar. Apparently, the increased steric bulk of the latter ligand can approximately compensate for the strong coordinating capability of the N(lutidine) donor atom of the BDPPpyr ligand. We attribute the enhanced steric shielding of the BDPPoxyl ligand also to its backbone conformation, with the xylene ring bending toward the metal center and hence sterically blocking one side of the complex.

Methyl Methacrylate Polymerization. Achiral and chiral lanthanidocene(III) complexes of type “Cp₂Ln–R” are highly efficient precatalysts for the stereoregular polymerization of methyl methacrylate (MMA).³⁵ The steric bulk and basicity/nucleophilicity of the operational Ln–R functionality, adding to MMA via 1,4-addition (enolate formation), is of utmost importance for controlling stereoregulation, molecular weight, and polydispersity. Hydrido,³⁶ hydrocarbyl,³⁷ amido,³⁸ and sulfido moieties³⁹ were shown to display efficient groups R for polymerization initiation. All of the monoalkyl and heteroleptic amide complexes **7–14** reported in this paper were examined in MMA polymerization. The polymerizations were carried out in toluene at 40 °C. After the mixture was stirred for 48 h, the reaction was quenched with methanol and the precipitated polymer was collected by filtration and dried under reduced pressure.

Interestingly, only the BDPPpyr (**1**)-derived complexes were found to catalyze the polymerization of MMA. The analytical data of the PMMA obtained are summarized in Table 3. The scandium complexes **7a**, **9a**, and **10a** showed very promising polymerization behavior (entries 1, 4, and 5). Both initiating alkyl and amide groups gave polymethyl methacrylate with nar-

Table 3. Polymerization of Methyl Methacrylate Catalyzed by Rare-Earth Alkyl and Amido Complexes^a

entry	pre-cat.	conversn (%)	10 ^{−3} M _w (g/mol)	10 ^{−3} M _n (g/mol) ^b	M _w /M _n	tacticity ^c <i>mr</i> / <i>mm</i> / <i>rr</i>	T _g ^d (°C)
1	7a	95	129	81	1.60	44/6.5/49.5	77
2	7b	11	5149	60	86.5	27/20/53	
3	7c	12	1720	58	29.9	25/37/38	
4	9a	87	83	65	1.28	49.5/9/41.5	84
5	10a	>99	105	67	1.56	47.5/8/44.5	99
6	10b	trace	1837	105	17.5	21/19.5/59.5	

^a Conditions: in toluene; precat./MMA (mol/mol) = 1/500; MMA/solvent (v/v) = 1/10; polymerization time 48 h; polymerization temperature 40 °C. ^b Measured by GPC calibrated with standard polystyrene samples. ^c *mr*, *mm*, and *rr* are hetero-, iso-, and syndiotactic triads, respectively. ^d Glass temperature.

row polydispersity indicative of a living polymerization (M_w/M_n = 1.28 for **9a**; for an ideal living polymerization M_n = 50 × 10³ g/mol). In contrast, corresponding complexes of the larger metal centers lutetium and yttrium showed negligible monomer conversion, giving polymers of very broad polydispersities (entries 2, 3, and 6). Apparently, the BDPPpyr ligand optimally matches the stereoelectronic demands of the Sc(III) center as a true ancillary ligand, its chelating Sc–N bonds behaving passively in the initiation and propagation process. The polymer microstructure as judged by ¹³C NMR spectroscopy is predominantly syndio- (ca. 50%) and heterotactic (ca. 50%). The initiator behavior of complexes **7** and **8** bearing the BDPPpyr ligand shows that steric unsaturation, when it implies enhanced complex instability (larger metal centers!), counteracts catalytic activity. Also, the nonactive BMespyr-derived complexes **11** and **12** point toward the importance of steric shielding of the metal center and/or steric shielding of the Ln–N(diamide) bonds. Furthermore, complex symmetry and/or the presence of additional donor atoms, expressed in a formally increased coordination number, seem to be crucial, as shown for the lack of polymerization capability of four-coordinate BDPPoxyl-derived complexes **14**. Note that the influence of the initiating ligand, alkyl vs amide, seems to be marginal.

Conclusions

Functionalized [NNN]^{2−} diamide ligands such as 2,6-bis(((2,6-diisopropylphenyl)amido)methyl)pyridine (BDPPpyr) provide versatile ancillary ligand sets for rare-earth-based post-metallocene complexes. The use of a series of structurally related ligands showed that the formation of the diamide complexes via alkane and amine elimination routes, their stability, and catalytic reactivity are sensitively balanced by stereoelectronic factors. An optimal coordinative fit of the *n*-chelating ligand (bite angle) and metal size are crucial. The steric shielding of the metal center by the ancillary ligand periphery and by additional donor solvent molecules has also a marked effect on complex stability and reactivity. Moreover, the catalytic performance of such heteroleptic diamide-supported complexes in methyl methacrylate polymerization revealed the coordination geometry to be an important factor as well. Accordingly, low coordination numbers (steric unsaturation) do not seem to be the prevalent steric criterion for enhanced catalytic activity of organo-rare-earth complexes.

(35) (a) Yasuda, H.; Tamai, H. *Prog. Polym. Sci.* **1993**, *18*, 1097. (b) Yasuda, H.; Ihara, E. *Macromol. Chem. Phys.* **1995**, *196*, 2417. (c) Yasuda, H.; Ihara, E.; Hayakawa, T.; Kakehi, T. *J. Macromol. Symp.—Pure Appl. Chem.* **1997**, *A34*, 1929.

(36) (a) Yasuda, H.; Yakamoto, H.; Yokota, K.; Miyake, S.; Nakamura, A. *J. Am. Chem. Soc.* **1992**, *114*, 4908. (b) Yasuda, H.; Yakamoto, H.; Yamashita, M.; Yokota, K.; Nakamura, A.; Miyake, S.; Kai, Y.; Kanehisa, N. *Macromolecules* **1993**, *26*, 7134.

(37) Giardello, M. A.; Yamamoto, Y.; Brard, L.; Marks, T. J. *J. Am. Chem. Soc.* **1995**, *117*, 3276.

(38) (a) Mao, L.; Shen, Q.; Sun, J. *J. Organomet. Chem.* **1998**, *566*, 9. (b) Mao, L.; Shen, Q. *J. Polym. Sci., Part A: Polym. Chem.* **1998**, *36*, 1593. (c) Lee, M. H.; Hwang, K.-W.; Kim, Y.; Kim, J.; Han, Y.; Do, Y. *Organometallics* **1999**, *18*, 5124. (d) Qian, C.; Nie, W.; Sun, J. *Organometallics* **2000**, *19*, 4134. (e) Qian, C.; Zou, G.; Chen, Y.; Sun, J. *Organometallics* **2001**, *20*, 3106.

(39) Nakayama, Y.; Shibahara, T.; Fukumoto, H.; Nakamura, A.; Mashima, K. *Macromolecules* **1996**, *29*, 8014.

Experimental Section

General Procedures. Unless otherwise indicated, all reactions and manipulations with air-sensitive compounds were performed under dry argon, using standard Schlenk and glovebox techniques. Reagents were obtained from commercial suppliers and used without further purification, unless otherwise noted. Hexane and toluene were degassed and then dried using a method described by Grubbs et al.⁴⁰ THF was distilled from Na/K alloy benzophenone ketyl. Solvents were stored in a glovebox. Deuterated solvents were distilled from Na/K alloy and stored in a glovebox over activated 4 Å molecular sieves. $\text{LnCl}_3(\text{THF})_x$ ²² and $\text{LiCH}_2\text{SiMe}_3$ ^{25c} were prepared according to literature procedures. A slightly modified procedure was used for the preparation of the complexes $\text{Ln}(\text{CH}_2\text{SiMe}_3)_3(\text{THF})_2$ (**5**).²³ 2,6-Bis(((2,6-diisopropylphenyl)amino)methyl)pyridine ($\text{H}_2\text{BDPPpyr}$, **1**) was prepared by using a method described by McConville.²⁰ Organolithiations were carried out according to standard literature methods. Methyl methacrylate was dried using a method described previously.⁴¹ ¹H NMR spectra were recorded on a Bruker DPX-400 (FT, 400 MHz ¹H; 100 MHz ¹³C) spectrometer. Chemical shifts are reported in ppm relative to TMS (¹H, ¹³C, and ²⁹Si) at room temperature; *J* values are given in Hz. IR spectra were recorded on a Perkin-Elmer 1650 FT-IR spectrometer as Nujol mulls. Elemental analyses were performed in the microanalytical laboratory of the institute. Some carbon analyses were found outside journal guidelines, which could be due to the presence of fractional amounts of solvent (**2**, **3** (=oil)) and an instability at ambient temperature due to the presence of intrinsically labile alkyl and isopropylamide moieties (**5b**, **6a**, **6b**, **7a**, **7b**, **9a**). Incomplete combustion of the samples, particularly for the element combination Ln/N/Si (**8b**, **12a**), has also been discussed to explain the mismatch of the elemental analyses of organolanthanide compounds.⁴⁷

2,6-Bis((mesitylamino)methyl)pyridine ($\text{H}_2\text{BMespyr}$, **2).** A THF solution of 1.13 g of lithium 2,4,6-trimethylanilide (8 mmol, 35 mL) was added slowly to a stirred solution of 1.06 g of 2,6-bis(bromomethyl)pyridine (4 mmol) in THF (15 mL) at -78°C . The mixture was warmed to ambient temperature and stirred for 16 h. The solution was quenched with a saturated NaHCO_3 solution (50 mL) and extracted with ether (50 mL). The solvent was removed in vacuo, and the resulting solid was dissolved in 50 mL of hexane and filtered. Solvent removal and drying under reduced pressure yielded 852 mg (57%) of a white solid. ¹H NMR (400 MHz, C_6D_6): δ 7.35 (dd, 1H, pyr), 7.2–7.1 (m, 4H, ar), 7.04 (d, 2H, pyr), 4.75 (s br, 2H, N–H), 4.53 (s, 4H, N–CH₂), 2.63 (s, 12H, ar-CH₃), 2.53 (s, 6H, ar-CH₃). ¹³C NMR (100 MHz, C_6D_6): δ 159.2, 144.1, 136.7, 131.2, 129.9, 120.3 (C_{ar}), 54.3 (N–CH₂), 20.7 (ar-CH₃), 18.7 (ar-CH₃). IR: ν 3355 (m, N–H), 2741 (m), 1590 (s), 1575 (m), 1538 (w), 1481 (s), 1458 (vs, Nujol), 1374 (s, Nujol), 1303 (m), 1258 (m), 1229 (w), 1154 (m), 1083 (m), 1031 (m), 852 (s), 799 (w), 720 (m), 561 (w), 539 (w), 505 (w), 488 (w), 466 (w), 452 (w), 434 (w), 427 (w), 417 (w) cm^{-1} . Anal. Calcd for $\text{C}_{25}\text{H}_{31}\text{N}_3$: C, 80.4; H, 8.4; N, 11.2. Found: C, 79.4; H, 8.3; N, 10.8.

1,3-Bis(((2,6-diisopropylphenyl)amino)methyl)benzene ($\text{H}_2\text{BDPPmxy}$, **3).** To a stirred solution of 486 mg of α,α' -dibromo-*m*-xylene (1.84 mmol) in 5 mL of THF at ambient temperature was added a solution of 709 mg of lithium 2,6-diisopropylanilide (3.93 mmol) in 5 mL of THF. The solution was stirred for 18 h, and the solvent was removed in vacuo. The resulting yellow oil was dissolved in 15 mL of hexane. A white precipitate formed, which was separated by filtration and extracted with hexane. The remaining hexane phases were combined and the solvent was removed under reduced pressure to yield 773 mg (92%) of a colorless oil. ¹H NMR (400 MHz,

C_6D_6): δ 7.59 (s br, 1H, ar), 7.33 (m, 2H, ar), 7.26–7.13 (m, 6H, ar), 4.08 (d, ³*J* = 7.0 Hz 4H, N–CH₂), 3.37 (sp, ³*J* = 6.9 Hz, 4H, ar-CH), 3.17 (t, ³*J* = 7.0 Hz, 2H, N–H), 1.22 (d, ³*J* = 6.9 Hz, 24H, CH₃). ¹³C NMR (100 MHz, C_6D_6): δ 143.4, 143.1, 141.1, 129.1, 127.4, 127.0, 124.7, 124.0 (C_{ar}), 56.4 (N–CH₂), 28.1 (ar-CH), 24.4 (CH₃). IR: ν 3374 (m, N–H), 1609 (w), 1589 (w), 1461 (vs, Nujol), 1378 (s, Nujol), 1362 (s), 1332 (m), 1310 (m), 1255 (s), 1244 (s), 1192 (s), 1159 (w), 1110 (m), 1055 (s), 995 (w), 967 (w), 932 (m), 899 (w), 888 (w), 863 (w), 847 (w), 800 (m), 786 (m), 770 (m), 756 (s), 745 (s), 721 (m), 710 (s), 701 (s), 663 (w), 652 (w), 625 (w), 611 (w), 567 (w), 553 (w), 526 (m), 518 (w), 493 (w), 477 (w), 452 (w), 433 (m), 408 (w) cm^{-1} . Anal. Calcd for $\text{C}_{32}\text{H}_{44}\text{N}_2$: C, 84.2; H, 9.7; N, 6.1. Found: C, 82.5; H, 9.6; N, 5.8.

1,2-Bis(((2,6-diisopropylphenyl)amino)methyl)benzene ($\text{H}_2\text{BDPPoxy}$, **4).** To a stirred solution of 494 mg of α,α' -dibromo-*o*-xylene (1.87 mmol) in 5 mL of THF was added a solution of 721 mg of lithium 2,6-diisopropylanilide (3.93 mmol) in 5 mL of THF at ambient temperature. The solution was stirred for 18 h, and the solvent was removed in vacuo. The resulting yellow oil was dissolved in 15 mL of hexane, and a white precipitate formed, which was separated by filtration and extracted with hexane. The remaining hexane phases were combined, and the solvent was removed under reduced pressure to yield 769 mg (90%) of an orange powder. ¹H NMR (400 MHz, C_6D_6): δ 7.55 (m, 2H, ar), 7.2–7.1 (m, 8H, ar), 4.23 (d, 4H, N–CH₂), 3.37 (sp, ³*J* = 6.9 Hz, 4H, ar-CH), 1.21 (d, ³*J* = 6.9 Hz, 24H, CH₃). ¹³C NMR (100 MHz, C_6D_6): δ 143.7, 143.0, 138.6, 128.9, 127.9, 124.7, 124.0 (C_{ar}), 54.0 (N–CH₂), 28.2 (ar-CH), 24.4 (CH₃). IR: ν 3355 (m N–H), 2722 (m), 2677 (w), 1914 (w), 1853 (w), 1792 (w), 1588 (m), 1458 (vs Nujol), 1377 (vs Nujol), 1362 (s), 1338 (s), 1310 (s), 1254 (s), 1220 (m), 1192 (s), 1110 (m), 1053 (s), 964 (w), 932 (s), 889 (w), 804 (s), 743 (vs), 677 (w), 605 (w), 576 (w), 528 (w) cm^{-1} . Anal. Calcd for $\text{C}_{32}\text{H}_{44}\text{N}_2$: C, 84.2; H, 9.7; N, 6.1. Found: C, 84.4; H, 9.3; N, 5.8.

General Procedure for Synthesizing $\text{Ln}(\text{CH}_2\text{SiMe}_3)_3(\text{THF})_2$ (5**).** To a suspension of $\text{LnCl}_3(\text{THF})_x$ in 5 mL of hexane was added dropwise a solution of $\text{LiCH}_2\text{SiMe}_3$ in 13 mL of hexane at ambient temperature. The mixture was stirred for 3 h and then filtered. The solid residue was extracted with 10 mL of hexane, and the volatiles were removed in vacuo, giving a white solid. The product was recrystallized from a minimum amount of hexane at -30°C , yielding the pure product as colorless crystals. **5a**: 620 mg of $\text{ScCl}_3(\text{THF})_3$ (1.69 mmol); 468 mg of $\text{LiCH}_2\text{SiMe}_3$ (4.97 mmol); yield 505 mg (71%). Anal. Calcd for $\text{C}_{20}\text{H}_{49}\text{O}_2\text{ScSi}_3$: C, 53.3; H, 11.0. Found: C, 53.7; H, 10.8. **5b**: 851 mg of $\text{LuCl}_3(\text{THF})_3$ (1.71 mmol); 474 mg of $\text{LiCH}_2\text{SiMe}_3$ (5.04 mmol); yield 646 mg (65%). Anal. Calcd for $\text{C}_{20}\text{H}_{49}\text{O}_2\text{LuSi}_3$: C, 41.4; H, 8.5. Found: C, 42.0; H, 8.9. **5c**: 752 mg of $\text{YCl}_3(\text{THF})_{3.5}$ (1.68 mmol); 466 mg of $\text{LiCH}_2\text{SiMe}_3$ (4.96 mmol); yield 574 mg (69%). Anal. Calcd for $\text{C}_{20}\text{H}_{49}\text{O}_2\text{YSi}_3$: C, 48.6; H, 10.0. Found: C, 48.7; H, 10.8. The spectroscopic data of complexes **5** correspond to those reported previously.²³

General Procedure for Synthesizing $\text{Ln}(\text{N}^i\text{Pr}_2)_3(\text{THF})_x$ (6**).** HN^iPr_2 was added to a stirred solution of $\text{Ln}(\text{CH}_2\text{SiMe}_3)_3(\text{THF})_2$ in 5 mL of hexane at ambient temperature and reacted for 18 h. Then the solution was filtered and the volatiles were removed in vacuo. The resulting yellow solid was recrystallized from hexane to yield the pure product as colorless crystals.

$\text{Sc}(\text{N}^i\text{Pr}_2)_3(\text{THF})$ (6a**):** 240 mg of $\text{Sc}(\text{CH}_2\text{SiMe}_3)_3(\text{THF})_2$ (0.53 mmol); 164 mg of HN^iPr_2 (1.62 mmol); yield 155 mg (70%). ¹H NMR (400 MHz, C_6D_6): δ 3.82 (m, 4H, THF), 3.66 (sp, ³*J* = 6.4 Hz, 6H, N–CH), 1.37 (d, ³*J* = 6.4 Hz, 36H, CH₃), 1.17 (m, 4H, THF). ¹³C NMR (100 MHz, C_6D_6): δ 72.4 (THF), 47.1 (N–CH), 27.0 (CH₃) 24.9 (THF). Anal. Calcd for $\text{C}_{22}\text{H}_{50}\text{ON}_3\text{Sc}$: C, 63.3; H, 12.1; N, 10.1. Found: C, 62.6; H, 11.7; N, 9.9.

$\text{Lu}(\text{N}^i\text{Pr}_2)_3(\text{THF})$ (6b**).** 295 mg $\text{Lu}(\text{CH}_2\text{SiMe}_3)_3(\text{THF})_2$ (0.51 mmol); 157 mg HN^iPr_2 (1.56 mmol); yield 212 mg (76%). ¹H

(40) Grubbs, R. H.; Pangborn, A. B.; Giardello, M. A.; Rosen, R. K.; Timmers, F. J. *Organometallics* **1996**, *15*, 1518.

(41) Allen, R. D.; Long, T. E.; McGrath, J. E. *Polym. Bull.* **1986**, *15*, 127.

NMR (400 MHz, C_6D_6): δ 3.72 (m, 4H, THF), 3.63 (sp, $^3J = 6.3$ Hz, 6H, N-CH), 1.39 (d, $^3J = 6.3$ Hz, 36H, CH_3), 1.13 (m, 4H, THF). ^{13}C NMR (100 MHz, C_6D_6): δ 72.3 (THF), 47.3 (N-CH), 27.0 (CH_3) 24.8 (THF). Anal. Calcd for $C_{22}H_{50}LuON_3$: C, 48.3; H, 9.2; N, 7.7. Found: C, 48.9; H, 9.1; N, 7.3.

$Y(NiPr)_2(THF)_2$ (6c): 283 mg of $Y(CH_2SiMe_3)_3(THF)_2$ (0.57 mmol); 176 mg of $HNiPr_2$ (1.77 mmol); yield 246 mg (81%). 1H NMR (400 MHz, C_6D_6): δ 3.62 (m, 8H, THF), 3.56 (sp, $^3J = 6.4$ Hz, 6H, N-CH), 1.38 (d, $^3J = 6.4$ Hz, 36H, CH_3), 1.25 (m, 8H, THF). ^{13}C NMR (100 MHz, C_6D_6): δ 70.2 (THF), 47.6 (N-CH), 26.8 (CH_3) 25.2 (THF). Anal. Calcd for $C_{26}H_{58}O_2N_3Y$: C, 58.5; H, 11.0; N, 7.9. Found: C, 58.4; H, 10.8; N, 7.2.

(BDPPpyr)ScCH₂SiMe₃(THF) (7a). To a stirred solution of 296 mg of **1** (0.66 mmol) in 10 mL of THF was added dropwise a solution of 300 mg of **5a** (0.66 mmol) in 5 mL of THF at ambient temperature. The mixture was stirred for 1 h and filtered, and the volatiles were removed in vacuo, yielding 436 mg (>99%) of a yellow powder. Recrystallization from a mixture of hexane and toluene at -30 °C afforded colorless crystals suitable for an X-ray analysis. 1H NMR (400 MHz, C_6D_6): δ 7.22 (dd, 2H, ar), 7.12 (d, 4H, ar), 6.94 (dd, 1H, pyr), 6.60 (d, 2H, pyr), 5.41 (d, $^2J = 20.1$ Hz, 2H, N-CH₂), 4.54 (m, 2H, ar-CH), 4.46 (d, $^2J = 20.1$ Hz, 2H, N-CH₂), 3.43 (m, 2H, ar-CH), 3.01 (m, 4H, THF), 1.53 (d, 6H, CH_3), 1.45 (d, 6H, CH_3), 1.15 (d, 6H, CH_3), 1.14 (d, 6H, CH_3), 0.78 (m, 4H, THF), 0.16 (s, 9H, Si-CH₃), 0.05 (s, 2H, Sc-CH₂). ^{13}C NMR (100 MHz, C_6D_6): δ 163.8, 152.7, 147.4, 145.9, 137.2, 124.1, 123.7, 123.4, 117.4 (C_{ar}), 71.2 (THF), 64.5 (N-CH₂), 28.2, 27.2, 26.2, 25.7, 25.2, 24.7 (ar-CH, CH_3 , THF, Sc-CH₂), 3.7 (Si-CH₃). ^{29}Si NMR (79.43 MHz, C_6D_6): δ -4.3. Anal. Calcd for $C_{39}H_{66}N_3OScSi$: C, 71.0; H, 9.2; N, 6.4. Found: C, 70.2; H, 9.7; N, 5.7.

(BDPPpyr)LuCH₂SiMe₃(THF)₂ (7b). A solution of 272 mg of **5b** (0.47 mmol) in 5 mL of THF was added dropwise to a stirred solution of 214 mg of **1** (0.47 mmol) in 8 mL of THF at ambient temperature. The mixture was stirred for 1 h and then filtered, and the volatiles were removed in vacuo, resulting in a yellow powder. Recrystallization from a mixture of hexane and toluene at -30 °C yielded 282 mg (76%) of the pure product. 1H NMR (400 MHz, THF- d_8): δ 7.80 (dd, 1H, pyr), 7.29 (d, 2H, pyr), 7.03 (d, 4H, ar), 6.91 (dd, 2H, ar), 4.95 (s, 4H, N-CH₂), 3.84 (m, 4H, ar-CH), 1.16 (d, 12H, CH_3), 1.14 (d, 12H, CH_3), -0.27 (s, 9H, Si-CH₃), -0.82 (s, 2H, Lu-CH₂). ^{13}C NMR (100 MHz, THF- d_8): δ 165.7, 152.9, 147.8, 138.2, 123.9, 123.4, 118.5 (C_{ar}), 65.8 (N-CH₂), 27.9, 26.9, 26.4, 25.5 (ar-CH, CH_3 , Lu-CH₂), 4.1 (Si-CH₃). ^{29}Si NMR (79.43 MHz, THF- d_8): δ -1.1. Anal. Calcd for $C_{43}H_{68}LuN_3O_2Si$: C, 59.9; H, 8.0; N, 4.9. Found: C, 59.9; H, 7.9; N, 4.9.

(BDPPpyr)YCH₂SiMe₃(THF)₂ (7c). To a stirred solution of 221 mg of **1** (0.48 mmol) in 8 mL of THF was added dropwise a solution of 239 mg of **5c** (0.48 mmol) in 7 mL of THF at ambient temperature. The mixture was stirred for 1 h and filtered, and the volatiles were removed in vacuo, resulting in a brown powder. Recrystallization from a mixture of hexane and toluene at -30 °C yielded 64 mg (21%) of the pure product. 1H NMR (400 MHz, THF- d_8): δ 7.78 (dd, 1H, pyr), 7.27 (d, 2H, pyr), 7.03 (d, 4H, ar), 6.94 (dd, 2H, ar), 4.87 (s, 4H, N-CH₂), 3.80 (m, 4H, ar-CH), 1.17 (d, 12H, CH_3), 1.15 (d, 12H, CH_3), -0.27 (s, 9H, Si-CH₃), -0.73 (d, $^2J = 5.3$ Hz, 2H, Y-CH₂). ^{13}C NMR (100 MHz, THF- d_8): δ 165.8, 151.9, 147.9, 138.1, 123.9, 123.4, 118.4 (C_{ar}), 65.7 (N-CH₂), 28.0, 26.9, 26.4, 25.9 (ar-CH, CH_3 , Y-CH₂), 4.1 (Si-CH₃). Anal. Calcd for $C_{43}H_{68}N_3O_2SiY$: C, 66.6; H, 8.8; N, 5.4. Found: C, 66.5; H, 8.7; N, 5.2.

General Procedure for Synthesizing $LLn(THF)_2NR_2$ (8, 9, 12). To a stirred solution of the diamide-supported rare-earth alkyl complex in 5 mL of hexane was added HNR_2 at ambient temperature. The solution was stirred at ambient temperature for 18 h. Then the solution was filtered, and the volatiles were removed in vacuo. The resulting yellow solid was recrystallized from hexane to yield the pure product.

(BDPPpyr)LuN(SiHMe₂)₂(THF) (8b): 190 mg of **7b** (0.26 mmol); 46.8 μ L of bis(dimethylsilyl)amine (0.26 mmol); yield 180 mg (83%). 1H NMR (400 MHz, C_6D_6): δ 7.25 (dd, 2H, ar), 7.13 (d, 2H, ar), 6.95 (dd, 1H, pyr), 6.57 (d, 2H, pyr), 5.44 (d, $^2J = 19.0$ Hz, 2H, N-CH₂), 4.64 (m, 2H, Si-H), 4.49 (d, $^2J = 19.0$ Hz, 2H, N-CH₂), 4.35 (m, 2H, ar-CH), 3.54 (m, 2H, ar-CH), 3.07 (m, 4H, THF), 1.52 (d, 6H, CH_3), 1.44 (d, 6H, CH_3), 1.20 (d, 6H, CH_3), 1.13 (d, 6H, CH_3), 0.84 (m, 4H, THF), 0.29 (d, 12H, Si-CH₃). ^{13}C NMR (100 MHz, C_6D_6): δ 165.5, 155.4, 147.7, 146.5, 137.1, 124.0, 123.4, 122.9, 117.1 (C_{ar}), 70.9 (THF), 65.1 (N-CH₂), 28.5, 27.5, 26.2, 25.3, 24.9, 24.6 (ar-CH, CH_3 , THF), 4.3 (Si-CH₃). ^{29}Si NMR (79.43 MHz, C_6D_6): δ -22.7. IR: ν 2759 (m), 2672 (w), 2103 (m, Si-H), 2042 (m, Si-H), 1601 (m), 1574 (m), 1462 (vs, Nujol), 1377 (s, Nujol), 1308 (m), 1240 (s), 1202 (m), 1186 (w), 1157 (m), 1100 (w), 1052 (m), 1036 (m), 1004 (w), 940 (m), 893 (s), 858 (m), 836 (m), 773 (m), 721 (m), 678 (m), 624 (w), 543 (w), 515 (m), 483 (w), 472 (w), 452 (w), 444 (w), 436 (w), 430 (w), 408 (w) cm^{-1} . Anal. Calcd for $C_{39}H_{63}LuN_4OSi_2$: C, 56.1; H, 7.6; N, 6.7. Found: C, 57.1; H, 7.6; N, 6.0.

(BDPPpyr)YN(SiHMe₂)₂(THF)₂ (8c): 144 mg of **7c** (0.22 mmol); 42.6 μ L of bis(dimethylsilyl)amine (0.24 mmol); yield 134 mg (90%). 1H NMR (400 MHz, THF- d_8): δ 7.74 (dd, 1H, pyr), 7.19 (d, 2H, pyr), 7.00 (d, 4H, ar), 6.88 (m, 2H, ar), 4.78 (s, 4H, N-CH₂), 4.46 (m, 2H, Si-H), 3.67 (m, 4H, ar-CH), 1.18 (d, 12H, CH_3), 1.12 (d, 12H, CH_3), -0.08 (d, 12H, Si-CH₃). ^{13}C NMR (100 MHz, THF- d_8): δ 166.0, 154.7, 147.1, 138.0, 123.9, 122.9, 117.9 (C_{ar}), 65.8 (N-CH₂), 28.5, 26.9, 25.1 (ar-CH, CH_3), 4.0 (Si-CH₃). ^{29}Si NMR (79.43 MHz, THF- d_8): δ -22.9. IR: ν 2760 (m), 2672 (w), 2097 (H-Si, m), 2010 (H-Si, m), 1600 (w), 1574 (m), 1461 (vs, Nujol), 1421 (s), 1377 (vs), 1307 (s), 1239 (vs), 1201 (s), 1185 (m), 1157 (m), 1101 (m), 1052 (s), 1005 (m), 942 (s), 893 (vs), 855 (s), 836 (s), 804 (m), 773 (s), 722 (m), 688 (w), 624 (w), 542 (w), 474 (w), 421 (w), 409 (w) cm^{-1} . Anal. Calcd for $C_{43}H_{71}N_4O_2Si_2Y$: C, 62.9; H, 8.7; N, 6.8. Found: C, 63.2; H, 8.5; N, 6.7.

(BDPPpyr)ScNEt₂(THF) (9a): 206 mg of **7a** (0.31 mmol); 32.2 μ L of $HNEt_2$ (0.31 mmol); yield 162 mg (81%). 1H NMR (400 MHz, C_6D_6): δ 7.27 (dd, 2H, ar), 7.19 (d, 2H, ar), 6.93 (dd, 1H, pyr), 6.55 (d, 2H, pyr), 5.00 (d, $^2J = 19.4$ Hz, 2H, N-CH₂), 4.63 (d, $^2J = 19.4$ Hz, 2H, N-CH₂), 4.05 (m, 2H, ar-CH), 3.59 (sp, 2H, ar-CH), 3.34 (m, 4H, THF), 2.23 (q, 4H, N-CH₂Me), 1.44 (d, 6H, CH_3), 1.40 (d, 6H, CH_3), 1.27 (d, 6H, CH_3), 1.13 (d, 6H, CH_3), 0.98 (m, 4H, THF), 0.80 (t, 6H, NCH₂-CH₃). ^{13}C NMR (100 MHz, C_6D_6): δ 164.1, 155.0, 146.7, 145.6, 136.7, 123.9, 123.3, 123.0, 116.8 (C_{ar}), 71.1 (THF), 64.8 (N-CH₂), 41.9 (N-CH₂-Me), 27.5, 26.2, 25.3, 24.9, 24.6, 15.1 (ar-CH, CH_3 , N-CH₂-CH₃, THF). Anal. Calcd for $C_{39}H_{59}N_4OSc$: C, 72.6; H, 9.2; N, 8.7. Found: C, 71.9; H, 9.0; N, 8.5.

(BDPPpyr)LuNEt₂(THF) (9b): 182 mg of **7b** (0.23 mmol); 23.7 μ L of $HNEt_2$ (0.23 mmol); yield 155 mg (87%). 1H NMR (400 MHz, C_6D_6): δ 7.35-7.05 (m, 6H, ar), 6.93 (dd, 1H, pyr), 6.57 (d, 2H, pyr), 5.29 (d, $^2J = 19.6$ Hz, 2H, N-CH₂), 5.00 (d, $^2J = 19.6$ Hz, 2H, N-CH₂), 4.24 (m, 2H, ar-CH), 3.59 (m, 2H, ar-CH), 3.22 (q, 4H, N-CH₂Me), 3.11 (s, 4H, THF), 1.47 (m, 12H, CH_3), 1.23 (m, 12H, CH_3), 1.02 (t, 6H, NCH₂-CH₃), 0.91 (m, 4H, THF). ^{13}C NMR (100 MHz, C_6D_6): δ 165.2, 154.8, 147.6, 146.4, 136.8, 123.5, 123.3, 122.7, 117.1 (C_{ar}), 70.8 (THF), 65.5 (N-CH₂), 44.2 (N-CH₂Me), 28.3, 27.8, 27.1, 26.2, 25.4, 24.9 (ar-CH, CH_3 , N-CH₂-CH₃, THF). Anal. Calcd for $C_{39}H_{59}LuN_4O$: C, 60.5; H, 7.7; N, 7.2. Found: C, 60.2; H, 7.6; N, 6.5.

(BDPPpyr)YNEt₂(THF)₂ (9c): 162 mg of **7c** (0.26 mmol); 29.1 μ L of $HNEt_2$ (0.28 mmol); yield 168 mg (85%). 1H NMR (400 MHz, THF- d_8): δ 7.72 (dd, 1H, pyr), 7.20 (d, 2H, pyr), 7.00 (d, 4H, ar), 6.87 (dd, 2H, ar), 4.77 (s, 4H, N-CH₂), 3.58 (m, 4H, ar-CH), 2.60 (q, 4H, N-CH₂Me), 1.18 (d, 12H, CH_3), 1.16 (d, 12H, CH_3), 0.48 (t, 6H, NCH₂-CH₃). ^{13}C NMR (100 MHz, THF- d_8): δ 165.9, 154.3, 147.0, 137.6, 123.7, 122.7, 118.0 (C_{ar}), 66.4 (N-CH₂), 43.3 (N-CH₂Me), 30.6, 28.3, 26.7, 26.4,

16.3 (ar-CH, CH₃, N-CH₂-CH₃, THF). Anal. Calcd for C₄₃H₆₇N₄O₂Y: C, 67.9; H, 8.9; N, 7.4. Found: C, 68.0; H, 8.6; N, 7.7.

(BDPPpyr)ScN/Pr₂(THF) (10a). To a stirred solution of 209 mg of **1** (0.46 mmol) in 5 mL of hexane was added dropwise a solution of 191 mg of **6a** (0.46 mmol) in 10 mL of hexane at ambient temperature. The mixture was stirred for 7 h and filtered, and the volatiles were removed in vacuo, resulting in a yellow powder. Recrystallization from a mixture of hexane and toluene at -30 °C yielded 256 mg (79%) of the pure product. ¹H NMR (400 MHz, THF-*d*₈): δ 7.74 (dd, 1H, pyr), 7.19 (d, 2H, pyr), 6.97 (d, 4H, ar), 6.83 (dd, 2H, ar), 4.74 (m, 4H, N-CH₂), 3.81 (sp, 4H, N-CH), 1.14 (d, 12H, CH₃), 1.07 (d, 12H, CH₃), 1.00 (d, 12H, CH₃). ¹³C NMR (100 MHz, THF-*d*₈): δ 165.1, 156.6, 146.4, 138.0, 123.7, 122.5, 117.5 (C_{ar}), 64.6 (N-CH₂), 49.3 (N-CH), 30.5, 28.1, 27.0, 26.3 (ar-CH, CH₃). Anal. Calcd for C₄₁H₆₃N₄O₂Sc: C, 73.2; H, 9.4; N, 8.3. Found: C, 73.1; H, 9.5; N, 7.9.

(BDPPpyr)LuN/Pr₂(THF) (10b). A solution of 167 mg of **6b** (0.30 mmol) in 5 mL of hexane was added slowly to a stirred solution of 140 mg of **1** (0.30 mmol) in 5 mL of hexane at ambient temperature. After the mixture was stirred for 7 h, the solution was filtered and the volatiles were removed in vacuo, giving a yellow powder. Recrystallization from a mixture of hexane and toluene at -30 °C yielded 166 mg (71%) of the pure product. ¹H NMR (400 MHz, THF-*d*₈): δ 7.73 (dd, 1H, pyr), 7.18 (d, 2H, pyr), 6.98 (d, 4H, ar), 6.83 (dd, 2H, ar), 4.85 (s, 4H, N-CH₂), 3.78 (sp, 4H, ar-CH), 3.40 (sp, 2H, N-CH), 1.15 (d, 12H, CH₃), 1.10 (d, 12H, CH₃), 0.98 (d, 12H, CH₃). ¹³C NMR (100 MHz, THF-*d*₈): δ 166.0, 156.9, 147.0, 137.9, 123.7, 122.3, 117.7 (C_{ar}), 65.5 (N-CH₂), 48.2 (N-CH), 28.2, 27.5, 26.8, 26.3 (ar-CH, CH₃). Anal. Calcd for C₄₁H₆₃-LuN₄O: C, 61.3; H, 7.9; N, 7.0. Found: C, 60.9; H, 8.0; N, 6.6.

(BMespyr)ScCH₂SiMe₃(THF) (11a). To a stirred solution of 314 mg of **2** (0.84 mmol) in 8 mL of THF was slowly added a solution of 379 mg of **5a** (0.84 mmol) in 7 mL of THF at ambient temperature. The mixture was stirred for 15 min and then filtered, and the volatiles were removed in vacuo, resulting in a yellow powder. Recrystallization from a mixture of hexane and toluene at -30 °C yielded 208 mg (43%) of the pure product. ¹H NMR (400 MHz, THF-*d*₈): δ 7.79 (dd, 1H, pyr), 7.28 (d, 2H, pyr), 6.78 (s, 4H, ar), 4.72 (s, 4H, N-CH₂), 2.24 (s, 12H, ar-CH₃), 2.16 (s, 6H, ar-CH₃), -0.32 (s, 9H, Si-CH₃), -0.33 (s, 2H, Sc-CH₂). ¹³C NMR (100 MHz, THF-*d*₈): δ 165.2, 152.9, 138.2, 135.7, 131.1, 129.3, 118.2 (C_{ar}), 62.0 (N-CH₂), 26.4 (Sc-CH₂), 20.9, 19.4 (ar-CH₃), 3.7 (Si-CH₃). ²⁹Si NMR (79.43 MHz, THF-*d*₈): δ 3.7. Anal. Calcd for C₃₃H₄₈N₃-OScSi: C, 68.8; H, 8.4; N, 7.3. Found: C, 68.5; H, 8.3; N, 6.9.

(BMespyr)LuCH₂SiMe₃(THF)₂ (11b). A solution of 233 mg of **5b** (0.40 mmol) in 5 mL of THF was slowly added to a stirred solution of 15 mg of **2** (0.40 mmol) in 5 mL of THF at ambient temperature. After the mixture was stirred for 15 min, the solution was filtered and the volatiles were removed in vacuo. The resulting brown powder was recrystallized from a mixture of hexane and toluene at -30 °C yielding 53 mg (21%) of the pure product. ¹H NMR (400 MHz, THF-*d*₈): δ 7.73 (dd, 1H, pyr), 7.22 (d, 2H, pyr), 6.76 (s, 4H, ar), 4.85 (s, 4H, N-CH₂), 2.26 (s, 12H, ar-CH₃), 2.15 (s, 6H, ar-CH₃), -0.34 (s, 9H, Si-CH₃), -1.15 (s, 2H, Lu-CH₂). ¹³C NMR (100 MHz, THF-*d*₈): δ 166.7, 153.5, 137.7, 135.7, 130.1, 129.5, 118.1 (C_{ar}), 63.2 (N-CH₂), 26.4 (Lu-CH₂), 20.9, 19.7 (ar-CH₃), 4.3 (Si-CH₃). ²⁹Si NMR (79.43 MHz, THF-*d*₈): δ 0.4. Anal. Calcd for C₃₇H₅₆LuN₃O₂Si: C, 57.1; H, 7.3; N, 5.4. Found: C, 57.0; H, 6.7; N, 5.6.

(BMespyr)ScN(SiHMe₂)₂(THF) (12a): 150 mg of **11a** (0.26 mmol); 55.5 μL of bis(dimethylsilyl)amine (41 mg, 0.32 mmol); yield 119 mg (74%). ¹H NMR (400 MHz, C₆D₆): δ 7.00–6.96 (m, 5H, ar + pyr), 6.57 (d, 2H, pyr), 4.83 (sp, 2H, Si-H), 4.59 (s br, 4H, N-CH₂), 3.49 (s br, 4H, THF), 2.45 (s, 12H, ar-CH₃), 2.26 (s, 6H, ar-CH₃), 0.96 (s br, 4H, THF), 0.11 (d, 12H, Si-CH₃). ¹³C NMR (100 MHz, C₆D₆): δ 164.6, 154.1, 136.7, 135.4,

130.9, 129.3, 116.8 (C_{ar}), 71.9 (THF), 62.4 (N-CH₂), 27.2, 21.2, 19.8 (ar-CH₃, THF), 3.5 (Si-CH₃). ²⁹Si NMR (79.43 MHz, C₆D₆): δ -20.7. IR: ν 2729 (s), 2662 (m), 2075 (m, Si-H), 1920 (w, Si-H), 1601 (w), 1573 (m), 1458 (vs, Nujol), 1376 (s, Nujol), 1340 (m), 1298 (m), 1242 (s), 1225 (s), 1182 (m), 1157 (m), 1028 (s), 935 (m), 898 (s), 845 (s), 796 (m), 763 (m), 726 (m), 695 (w), 626 (m), 590 (w), 523 (m), 505 (w), 490 (w), 472 (w), 454 (w), 437 (w), 424 (m), 413 (w), 403 (w) cm⁻¹. Anal. Calcd for C₃₃H₅₁N₄O₂ScSi₂: C, 63.8; H, 8.3; N, 9.0. Found: C, 63.0; H, 8.4; N, 8.5.

(BMespyr)LuN(SiHMe₂)₂(THF) (12b): 150 mg of **8b** (0.24 mmol); 44.1 μL of bis(dimethylsilyl)amine (33 mg 0.25 mmol); yield 141 mg (78%). ¹H NMR (400 MHz, THF-*d*₈): δ 7.73 (dd, 1H, pyr), 7.20 (d, 2H, pyr), 6.75 (s, 4H, ar), 4.77 (s, 4H, N-CH₂), 4.34 (m, 2H, Si-H), 2.25 (s, 12H, ar-CH₃), 2.15 (s, 6H, ar-CH₃), -0.16 (d, 12H, Si-CH₃). ¹³C NMR (100 MHz, C₆D₆): δ 165.7, 153.8, 136.7, 135.6, 130.2, 129.3, 117.1 (C_{ar}), 71.1 (THF), 62.7 (N-CH₂), 24.8, 21.0, 19.7 (ar-CH₃, THF), 3.7 (Si-CH₃). ²⁹Si NMR (79.43 MHz, C₆D₆): δ -22.2. IR: ν 2727 (m), 2667 (m), 2062 (m, Si-H), 1601 (w), 1574 (w), 1462 (vs, Nujol), 1376 (s, Nujol), 1297 (m), 1241 (s), 1204 (w), 1185 (w), 1157 (m), 1058 (m), 1027 (m), 942 (m), 895 (s), 852 (m), 838 (m), 789 (w), 768 (w), 721 (m), 680 (w), 621 (w), 596 (w), 562 (w), 530 (w), 515 (w), 482 (w), 472 (w), 455 (w), 439 (w), 415 (w) cm⁻¹. Anal. Calcd for C₃₃H₅₁LuN₄O₂ScSi₂: C, 52.8; H, 6.9; N, 7.5. Found: C, 52.3; H, 7.0; N, 6.9.

(BMespyr)ScN/Pr₂(THF) (13a). To a stirred solution of 110 mg of **2** (0.30 mmol) in 5 mL of hexane was added dropwise a solution of 123 mg of **6a** (0.30 mmol) in 5 mL of hexane at ambient temperature. The mixture was stirred for 1 h and filtered, and the volatiles were removed in vacuo, giving a gray powder. Recrystallization from a mixture of hexane and toluene at -30 °C yielded 83 mg (47%) of the pure product. ¹H NMR (400 MHz, THF-*d*₈): δ 7.70 (dd, 1H, pyr), 7.19 (d, 2H, pyr), 6.68 (s, 4H, ar), 4.63 (s, 4H, N-CH₂), 3.53 (sp, 4H, N-CH), 2.14 (s, 12H, ar-CH₃), 2.10 (s, 6H, ar-CH₃), 0.95 (d, 12H, CH₃). ¹³C NMR (100 MHz, THF-*d*₈): δ 165.6, 156.0, 137.9, 134.9, 129.5, 129.3, 117.7 (C_{ar}), 62.0 (N-CH₂), 48.0 (N-CH), 27.1, 20.7, 20.5 (ar-CH₃, CH₃). Anal. Calcd for C₃₅H₅₁N₄O₂Sc: C, 71.4; H, 8.7; N, 9.5. Found: C, 70.9; H, 9.0; N, 9.2.

(BDPPoxyl)ScCH₂SiMe₃(THF) (14a). To a stirred solution of 248 mg of **4** (0.54 mmol) in 5 mL of hexane was added dropwise a solution of 245 mg of **5a** (0.54 mmol) in 5 mL of hexane at ambient temperature. The mixture was stirred for 16 h and then filtered, and the volatiles were removed in vacuo, yielding 355 mg (>99%) of a yellow powder. Recrystallization from a mixture of hexane and toluene at -30 °C afforded colorless crystals suitable for an X-ray analysis. ¹H NMR (400 MHz, C₆D₆): δ 7.30 (m, 2H, ar), 7.24–7.18 (m, 6H, ar), 6.99 (m, 2H, ar), 5.52 (d, ²J = 12.0 Hz, 2H, N-CH₂), 4.26 (sp, 2H, ar-CH), 3.64 (d, ²J = 12.0 Hz, 2H, N-CH₂), 3.55 (sp, 2H, ar-CH), 3.28 (s br, 4H, THF), 1.62 (d, 6H, CH₃), 1.55 (d, 6H, CH₃), 1.34 (d, 6H, CH₃), 1.16 (d, 6H, CH₃), 1.15 (s br, 4H, THF), -0.25 (s, 9H, Si-CH₃), -0.30 (s, 2H, Sc-CH₂). ¹³C NMR (100 MHz, C₆D₆): δ 151.1, 145.9, 144.2, 142.1, 132.0, 124.7, 124.3, 123.5 (C_{ar}), 70.6 (THF), 60.8 (N-CH₂), 29.5, 27.9, 27.1, 25.8, 25.0, 24.7, (ar-CH, CH₃, THF, Sc-CH₂), 3.3 (Si-CH₃). ²⁹Si NMR (79.43 MHz, C₆D₆): δ -3.5. Anal. Calcd for C₄₀H₆₁N₂-OScSi: C, 72.9; H, 9.3; N, 4.3. Found: C, 72.4; H, 9.3; N, 4.2.

(BDPPoxyl)LuCH₂SiMe₃(THF) (14b). A solution of 265 mg of **5b** (0.46 mmol) in 5 mL of hexane was slowly added to a stirred solution of 208.7 mg of **4** (0.46 mmol) in 5 mL of hexane at ambient temperature. After the mixture was stirred for 16 h, the solution was filtered and the volatiles were removed in vacuo, yielding 362 mg (>99%) of a yellow powder. ¹H NMR (400 MHz, THF-*d*₈): δ 7.1–6.9 (m, 8H, ar), 6.88 (m, 2H, ar), 4.65 (s br, 4H, N-CH₂), 3.85 (s br, 4H, ar-CH), 1.22 (d, 24H, CH₃), -0.14 (s, 9H, Si-CH₃), -1.10 (s, 2H, Lu-CH₂). ¹³C NMR (100 MHz, THF-*d*₈): δ 155.2, 146.4, 142.1, 131.7, 127.6, 124.0, 122.9 (C_{ar}), 59.0 (N-CH₂), 28.7, 26.9, 26.4, (ar-CH, CH₃, Lu-CH₂), 4.3 (Si-CH₃). ²⁹Si NMR (79.43 MHz, THF-

Table 4. Crystal Data and Data Collection Parameters of Complexes 7a and 14a

	7a	14a
chem formula	C ₃₉ H ₆₀ N ₃ OScSi·C ₇ H ₈	C ₄₀ H ₆₁ N ₂ OScSi
fw	752.08	658.96
color/shape	colorless/fragment	colorless/fragment
cryst size (mm)	0.53 × 0.28 × 0.20	0.76 × 0.51 × 0.36
cryst syst	triclinic	monoclinic
space group	<i>P</i> $\bar{1}$ (No. 2)	<i>P</i> 2 ₁ (No. 4)
<i>a</i> (Å)	11.4010(1)	11.3658(1)
<i>b</i> (Å)	13.1150(2)	16.5331(2)
<i>c</i> (Å)	15.7320(2)	11.5392(1)
α (deg)	78.1150(7)	90
β (deg)	79.5690(8)	113.6789(5)
γ (deg)	76.8660(7)	90
<i>V</i> (Å ³)	2219.32(5)	1985.80(4)
<i>Z</i>	2	2
<i>T</i> (K)	193	153
ρ_{calcd} (g cm ⁻³)	1.125	1.102
μ (mm ⁻¹)	0.228	0.246
<i>F</i> ₀₀₀	816	716
θ range (deg)	2.13–27.50	3.13–25.35
data collected (<i>h</i> , <i>k</i> , <i>l</i>)	–14 to +14, –16 to +17, –19 to +20	–13 to +13, –19 to +19, –13 to +13
no. of rflns collected	17 191	38 508
no. of indep rflns/ <i>R</i> _{int}	9706 (all)/0.023	7256 (all)/0.043
no. of obsd rflns (<i>I</i> > 2 σ (<i>I</i>))	7529 (obsd)	6868 (obsd)
no. of params refined	537	650
<i>R</i> ₁ (obsd/all)	0.0426/0.0662	0.0273/0.0308
w <i>R</i> ₂ (obsd/all)	0.0973/0.1115	0.0638/0.0656
GOF (obsd/all)	1.099/1.099	1.033/1.033
max/min $\Delta\rho$ (e Å ⁻³)	+0.27/–0.35	+0.30/–0.15

*d*₈): δ 0.6. Anal. Calcd for C₄₀H₆₁LuN₂OSi: C, 60.9; H, 7.8; N, 3.6. Found: C, 60.5; H, 7.8; N, 3.5.

(BDPPoxyl)YCH₂SiMe₃(THF) (14c). To a stirred solution of 186 mg of **4** (0.41 mmol) in 5 mL of hexane was added dropwise a solution of 202 mg of **5c** (0.41 mmol) in 5 mL of hexane at ambient temperature. The mixture was stirred for 16 h and filtered, and the volatiles were removed in vacuo, yielding 287 mg (>99%) of a yellow powder. ¹H NMR (400 MHz, THF-*d*₈): δ 7.1–6.8 (m, 10H, ar), 4.69 (s br, 4H, N–CH₂), 3.78 (s br, 4H, ar–CH), 1.18 (d, 24H, CH₃), –0.01 (s, 9H, Si–CH₃), –0.96 (d, ²*J* = 3.6 Hz, 2H, Y–CH₂). ¹³C NMR (100 MHz, THF-*d*₈): δ 155.7, 146.3, 141.8, 131.0, 126.9, 124.0, 122.5 (C_{ar}), 58.7 (N–CH₂), 28.5, 26.9, 25.4, (ar–CH, CH₃, Y–CH₂), 4.5 (Si–CH₃). ²⁹Si NMR (79.43 MHz, THF-*d*₈): δ –1.7. Anal. Calcd for C₄₀H₆₁N₂OSiY: C, 68.3; H, 8.7; N, 4.0. Found: C, 67.8; H, 8.4; N, 3.6.

Polymerization of Methyl Methacrylate (MMA). In a typical reaction, to a solution of 0.2 mol % catalyst precursor in toluene (1 mL/mmol of MMA) was added the desired amount of MMA at ambient temperature. After the solution was stirred for 48 h at ambient temperature, the polymerization was terminated by the addition of 100 mL of methanol. The resulting white polymer was collected by filtration and dried under reduced pressure. The poly(methyl methacrylate) was

analyzed by means of gel permeation chromatography, NMR spectroscopy, and differential scanning calorimetry (cf. Table 3).

X-ray Structure Determinations of Complexes 7a and 14a. Crystals suitable for diffraction experiments were selected in a glovebox, coated with perfluorinated ether, and fixed in a capillary. Preliminary examination of the crystal quality and data collection were carried out on a Nonius KappaCCD diffractometer in combination with a rotating-anode X-ray generator and graphite-monochromated Mo K α radiation (λ = 0.710 73 Å) employing the COLLECT software package.⁴² A total of 604 (419) collected images were processed using Denzo.⁴³ Data for compound **14a** are given in parentheses. Absorption and/or decay effects were corrected during the scaling procedure.⁴³ The structures were solved by direct methods⁴⁴ and refined with standard difference Fourier techniques.⁴⁵ All non-hydrogen atoms of the asymmetric unit were refined with anisotropic thermal displacement parameters. In **14a** all hydrogen atoms were found in the difference Fourier maps and refined freely with individual isotropic thermal displacement. For **7a** all hydrogen atoms were placed in calculated positions and included in the structure factor calculation but not refined. Full-matrix least-squares refinements were carried out by minimizing $\sum w(F_o^2 - F_c^2)^2$ employing the SHELXL-97 weighting scheme and stopped at a maximum shift/error of <0.001 (0.001). The right enantiomer of **14a** is proven by the Flack parameter ϵ = –0.01(2). For the final model, 537 (650) parameters were refined to w*R*₂ = 0.1115 (0.0656) on the basis of all 9706 (7256) data. For details see Table 4.

Acknowledgment. We thank Degussa AG for generous financial support and polymer analysis. Support from the Deutsche Forschungsgemeinschaft, the Fonds der Chemischen Industrie, and Prof. Wolfgang A. Herrmann is gratefully acknowledged. F.E. thanks the Fonds der Chemischen Industrie for the award of a fellowship.

Supporting Information Available: Tables of X-ray crystallographic data for compounds **7a** and **14a**; these data are also given in CIF format. This material is available free of charge via the Internet at <http://pubs.acs.org>.

OM020783S

(42) Hooft, R. COLLECT, Data Collection Software for Nonius KappaCCD Devices; Nonius BV, Delft, The Netherlands, 1998.

(43) Otwinowski, Z.; Minor, W. In *Processing of X-ray Diffraction Data Collected in Oscillation Mode*; Carter, C. W., Jr., Sweet, R. M., Eds.; Academic Press: New York, 1997; Vol. 276, p 307.

(44) Altomare, A.; Cascarano, G.; Giacovazzo, C.; Guagliardi, A.; Burla, M. C.; Polidori, G.; Camalli, M. *J. Appl. Crystallogr.* **1994**, *27*, 435.

(45) Sheldrick, G. M. SHELXL-97; Universität Göttingen, Göttingen, Germany, 1998.

(46) Spek, A. L. PLATON, A Multipurpose Crystallographic Tool; Utrecht University: Utrecht, The Netherlands, 2001.

(47) Fryzuk, M. D.; Jafarpour, L.; Kerton, F. M.; Love, J. B.; Patrick, B. O.; Rettig, S. J. *Organometallics* **2001**, *20*, 1387.